

A ns-pulse Laser Microthruster

Claude R. Phipps¹, James R. Luke^{1,2}, Wesley Helgeson²
and Richard Johnson²

¹*Photonic Associates LLC, 200A Ojo de la Vaca Road, Santa Fe, New Mexico USA 87508*

Phone/Fax: 1-505-466-3877, Email: crhipps@aol.com

²*NMT/IERA, 901 University Blvd, Albuquerque, NM, USA 87106*

Abstract. We have developed a prototype device which demonstrates the feasibility of using ns-duration laser pulses in a laser microthruster. Relative to the ms-duration thrusters which we have demonstrated in the past, this change offers the use of any target material, the use of reflection-mode target illumination, and adjustable specific impulse. Specific impulse is adjusted by varying laser intensity on target. In this way, we were able to vary specific impulse from 200s to 3,200s on gold. We used a Concepts Research, Inc. microchip laser with 170mW average optical power, 8kHz repetition rate and 20 μ J pulse energy for many of the measurements. Thrust was in the 100nN - 1 μ N range for all the work, requiring development of an extremely sensitive, low-noise thrust stand. We will discuss the design of metallic fuel delivery systems. Ablation efficiency near 100% was observed. Results obtained on metallic fuel systems agreed with simulations. We also report time-of-flight measurements on ejected metal ions, which gave velocities up to 80km/s.

NOMENCLATURE

C_m = laser momentum coupling coefficient CW = “continuous wave”, continuous laser output rather than pulsed $DPSS$ = diode-pumped, solid state E = short for “10 [^] ” f = repetition frequency F = thrust g_o = acceleration of gravity at Earth’s surface I = laser intensity on target I_{sp} = specific impulse k = constant relating rotation angle θ to torque ksi = tensile strength expressed in klb/in ²	$\langle P \rangle$ = average incident laser power Q^* = specific ablation energy R = radius of thruster attachment point from center of rotation v_E = exhaust velocity TEC = thermoelectric cooler W = laser pulse energy incident on test sample Δm = ablated mass η_{AB} = ablation efficiency η_E = laser optical power out/electrical power in θ = angle of rotation of torsion bar τ = laser pulse duration
---	--

INTRODUCTION

Two difficulties were identified in earlier work in which we showed the feasibility of using ms-duration laser diodes to drive a microthruster based on ablation of solid polymer targets [1, 2]. One was the necessity of using polymer targets with low thermal conductivity such as PVC, PVN or GAP. For example, no metals could be used as targets because their thermal conductivity was too high to permit achievement of the temperatures necessary for efficient propulsion and minimally acceptable I_{sp} . The other problem was the requirement for transmission-mode illumination to avoid target ablation products backstreaming onto the optics [Figure 1]. Even though the transparent polymer layer in our tape targets is not penetrated by the laser-target interaction, some back-ablation does occur from the polyimide surface. It was always understood that ns-pulse illumination would eliminate both problems.

There was some concern about losing power conversion efficiency with this change. However, ns-pulse diode-pumped fiber laser amplifiers are now capable of wallplug-to-light efficiency $\eta_E > 40\%$ [3], so the conversion efficiency sacrifice is not prohibitive for the technology now, and may further improve in the future. Also, fiber lasers are low-mass devices, unlike conventional DPSS lasers.

In contrast, microchip lasers [4] currently have $\eta_E = 1-2\%$, a figure which is primarily due to the power consumed by the TEC which is required to stabilize the laser chip’s operating temperature.

The energetic advantages of ns-duration and shorter pulses for manipulating objects in space via laser ablation propulsion were pointed out in [5] and the possibility of using onboard microchip lasers for ns-duration propulsion was discussed in [4,6]. In [6], I_{sp} up to 4.9ks was reported using this technique. Other measurements going back several decades have shown [7,8] that I_{sp} values from 7 to more than 25ks can be obtained with simple desktop-scale ns-duration lasers using metallic targets in vacuum.

In this paper, we will describe measurements of thrust, specific impulse and energetic efficiency in laser propulsion with ns-duration pulses which were made for

Microthruster Illumination Summary

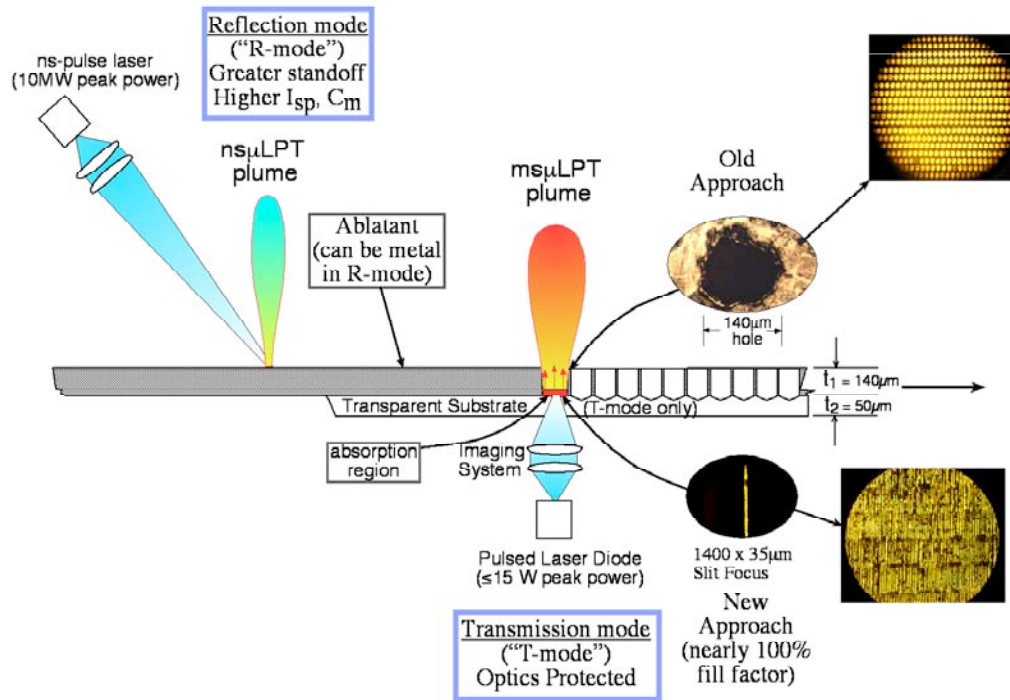


Figure 1. Transmission (T) vs. reflection (R) mode illumination. Nanosecond-pulse illumination permits using R-mode illumination in laser ablation propulsion, a definite advantage for simplicity of targets and optics, as well as laser energy deposition efficiency.

the first time using a completely self-contained microthruster suspended in a torsion-type thrust stand capable of 25nN precision in measuring thrust. Intensity on target was in the PW/m² range. Performance of the test stand is described in a companion paper in this conference.

TEST UNIT DESIGN

In order to test our concepts fully, it was necessary to build a test microthruster which could accommodate various target materials with features including a target delivery system providing several hours of operating lifetime, power supply and infrared data link, all completely self-contained and connected to the external world only through the torsion fiber which provided restoring force in the thrust-measurement apparatus [Figure 2]. The vacuum thrust stand setup was identical to the device reported in [1] except for a) 40-cm rather than 10-cm torsion fiber length, b) the critical damping attachment and c) the interferometer element in the center of the support bar. The latter replaces the simple mirror used as a rotation readout in [1]. The entire setup mounted inside our vacuum test chamber. Thrust F is given by $F = k\theta/R$, where $k = 194 \text{ nN-m}/\mu\text{rad}$ and $R = 0.155\text{m}$, so that $k/R = 1.25\text{nN}/\mu\text{rad}$. The rotation sensor

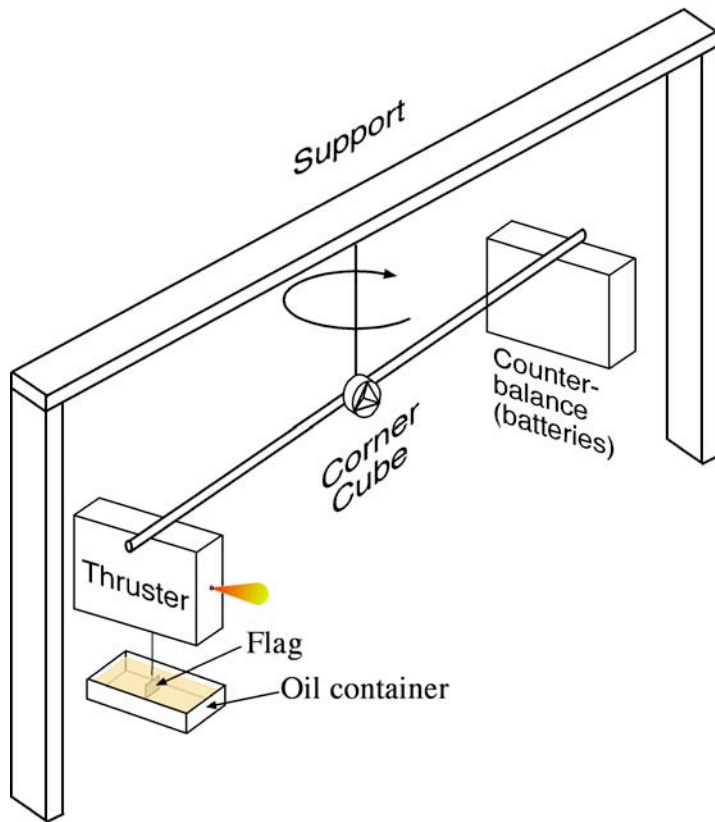


Figure 2. Vacuum thrust stand setup. Power supply is on board the thrust measurement bar with the thruster, and command and data transfer uses an IR data link, so that the only mechanical connection with the outside world is the 254- μm diameter steel fiber supporting the bar. An interferometer based on a solid glass retroreflecting “corner cube” (described below) is the key to resolving rotation of the bar. Critical damping

was seen with Zr coatings which were applied by ion sputtering, but Al coatings applied in this way were of good quality, although considerably thinner (1-2 μm vs. 20 μm). The causes of the problems with the Zr coatings have not been identified. We had the best results with gold electroplating. The coating was thick, tough and adherent, giving hours of good performance in tests (Fig. 4). A typical fuel disk would have lasted for 350 hours of continuous operation at the 10-100mW input optical power levels that we used for tests, or 5 hours at the 8W level we would propose for a space-qualified microthruster capable of generating 80 μN thrust.

Two different lasers were employed to provide the optical input for tests (Table 1). This was necessary because the Concepts Research microchip laser was incapable of generating the maximum intensities that we required. However, its 8kHz output format was the same as that of the fiber laser we plan to use in future work, and we felt

we developed was capable of resolving 20 μrad bar rotation and thus delivered 25nN precision.

A major design challenge was to develop a means of delivering laser energy to the system through the vacuum chamber envelope from two different benchtop laser systems while the apparatus was rotating in the test chamber. Our solution to this problem is shown in Figure 3.

Although operating conditions were sometimes deliberately chosen otherwise (e.g., for measurements of surface regularity obtained in laser planing of the surface), thrust data runs with the device were always set up with a radial scan speed sufficient to insure single-spot irradiation of any target site on the spinning fuel disk.

There have been some successes and some failures in our attempts to coat the disks. Delam-

that we should use it for as much of the data as possible. The Quantel laser was a standard flashlamp-pumped Nd:YAG tabletop unit.

To get the range of intensities we wanted to study, a beam from either of two lasers (Table 1)

Table 1. Target illumination parameters		
Laser	Quantel	Concepts Research
Pulse energy (mJ)	1-20	0.0132
Pulse repetition rate (Hz)	10	8000
Power on target (mW)	10-220	106
Beam quality factor M^2	3.6	1.2
Spot size on target (μm)	20-60	5-20
Fluence on target (J/m^2)	3E6-6E7	1-3E5
Pulse duration (ns)	4.55	4.0
Intensity on target (TW/m^2)	660-14,000	20-65
Typical radial velocity ($\mu\text{m}/\text{hr}$)	700	

was focused on the target by a 15-mm focal length lens. Beam incidence angle on the disk was 45 degrees. Spot sizes on target varied, as did the laser pulse energy, which was controlled by absorptive attenuators. Given the M^2 value for the Quantel laser (Table 1), the smallest spot we could expect was $20\mu\text{m}$. Typical laser spot diameter on target was

$40\mu\text{m}$, determined by microscopic examination.

An optical link operated through the vacuum chamber wall to turn the disk drive on and off, and commanded the transverse drive to move the lens across the disk in a radial direction at a velocity v_r which could be adjusted from $1\mu\text{m}/\text{hr}$ to $8,000\mu\text{m}/\text{hr}$. This was normally set to about $700\mu\text{m}/\text{hr}$ to avoid overlap even for our largest illumination spots. We developed a Labview® interface for the optical link.

The disk drive motor was operated by a bank of Li-ion batteries which also served as counterweight for the thruster. These were capable of powering the system, including the



Figure 3. Jet from an operating gold-coated target. Electroplating worked better than ion sputtering for applying the coatings, both for achieving thick ($25\mu\text{m}$) coatings and for causing less coating mechanical stress.

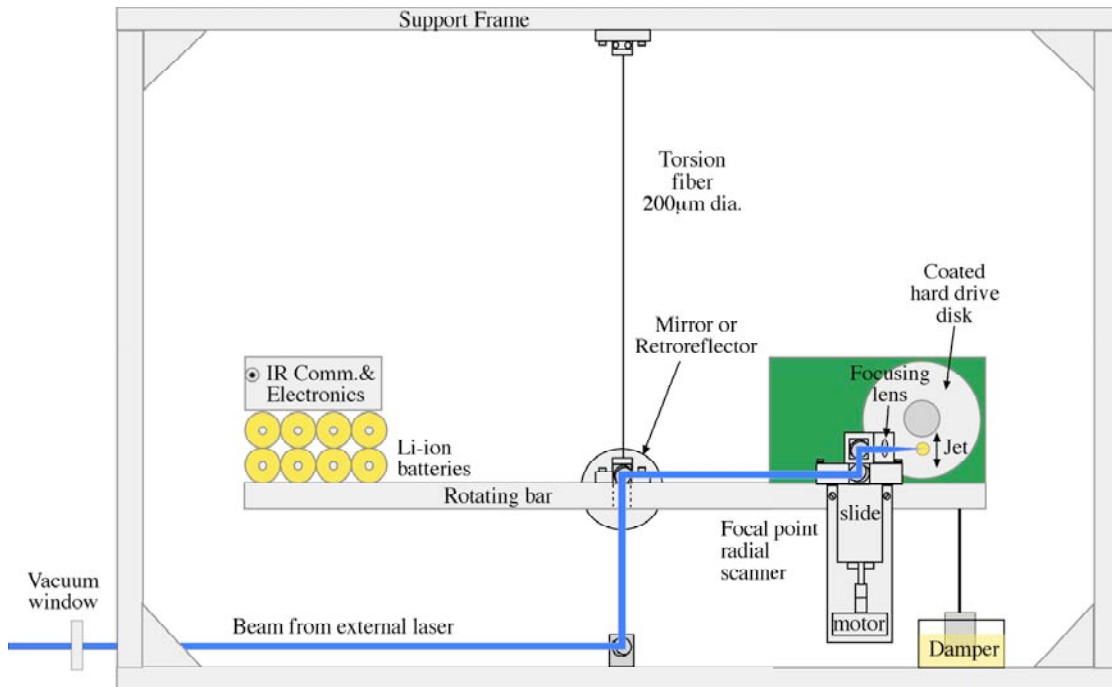


Figure 4. Design for ns-pulse thrust measurements. The steel fiber which was the core of the instrument was a 40-cm long strand of 250 μm , 500ksi steel “rocket wire” provided by MJ Wire, Inc. The hard drive was an IBM DKLA 22160 with a 2.5 inch diameter disk operating at 4200 rpm. An IR communication link with a Labview® interface that we developed handled data and commands. Input optical power levels ranged from 10 to 100mW. Mirrors at the center of rotation were needed to avoid beam misalignment as the torsion pendulum rotated. The motorized translation stage shown at right scanned the focal point across the disk.

transverse drive and the optical communication link, for up to three hours.

We found that it was necessary to momentarily turn the transverse drive stepper motor off when measuring thrust, because of the interaction between the motor’s magnetic field and the Earth’s field. Typical operating pressure for tests was 30 μtorr .

We installed a pair of shielded Langmuir/ Faraday time-of-flight (TOF) detectors in the chamber as shown in Figure 5. For all the work reported here, the dimensions d and s were 5.8 and 2.8 cm, respectively.

RESULTS

TOF data is presented in Figures 6 and 7, and tabulated in Table 2. Our choices of probe separation gave good signal strength and still provided adequate velocity resolution for the ion speeds we expected to find, in the range $2\text{E}4 < v_1 < 1\text{E}5$ m/s [$2\text{E}3 < I_{sp} < 1\text{E}4$]. For ion velocity measurements, we biased the probes so that only ions were collected. We found that $V = -10\text{V}$ was sufficient to do this. The two signals were recorded on a Tektronix 3014B digital storage oscilloscope.

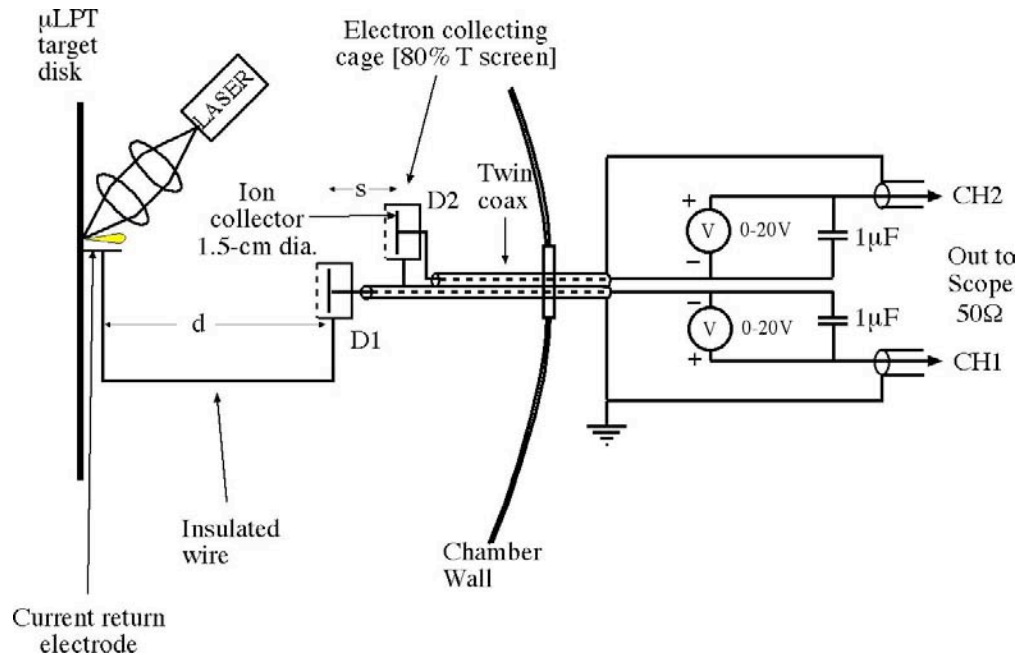


Figure 5. Twin Ion Time-of-flight Detectors were typically maintained at -10V bias to select ions and reject electrons to the 80% transmission screen covering the detector. A current return electrode was necessary because the source (the jet) is not grounded. Distance d is the separation of D1 from the source (5.8cm) and s is the mutual separation between D1 and D2 (2.8cm).

Table 2. Experimental results from representative tests				
Material	Gold		Aluminum	
Fluence (J/m^2)	6.36E5	2.08E7	3.46E5	1.08E5
Intensity (W/m^2)	1.40E14	4.57E15	7.60E13	2.37E13
Thrust (μN)	0.63	0.47	0.94	1.88
C_m ($\mu\text{N}/\text{W}$)	68	7.2	111	32
Q^* (kJ/kg)	5.28E5	5.90E5	9.79E4	2.71E5
I_{sp} (s) from $C_m Q^*$	3660	212	1120	520
η_{AB} (%)	100	0.75	61	8.1
Test duration (m)	120	16	120	24.25
v_i from TOF (m/s)	3.59E4	7.75E4	6.48E4	8.05E3
I_{sp} from v_i	3664	7905	6610	822
Test ID	BT12§	BT8§	9A§	4§, 17§

Figure 6 shows a typical TOF trace for moderate laser fluence. Figure 7 shows a high-fluence TOF trace.

Figures 8 and 9 show the results we obtained for thrust, C_m , I_{sp} and η_{AB} for the Al and Au target disks vs. fluence. Simulations that we did of the laser target interaction gave essentially

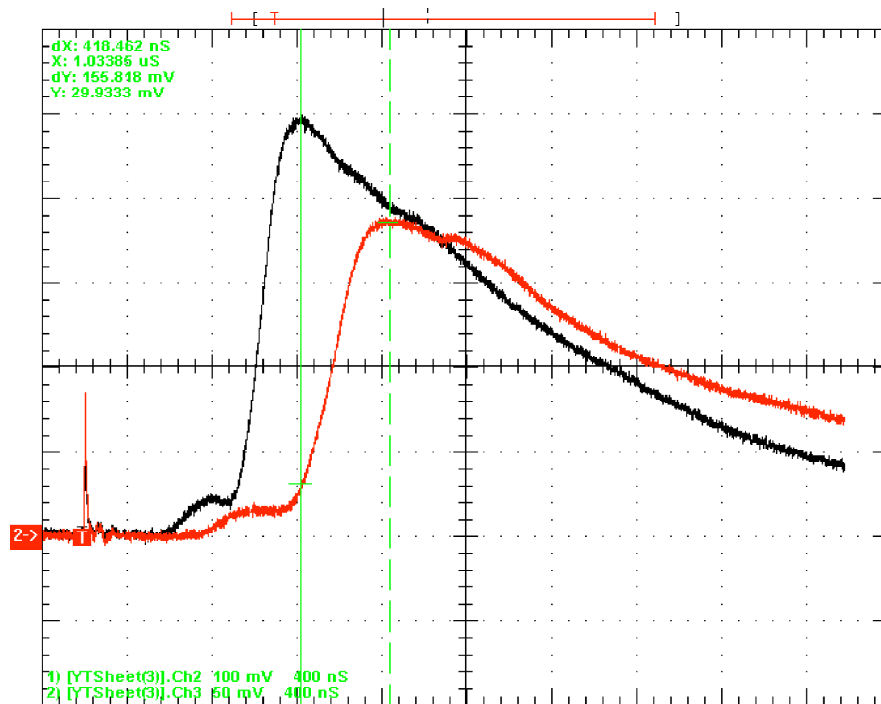


Figure 6. Moderate Fluence TOF Detector Trace (-10V bias, Au Target) shows ion speed 67km/s at the waveform peaks and 76km/s at the half-height of the rise. The two traces are derived from D1 and D2 in Figure 5, which are separated by 2.8cm. This corresponds to ion $I_{sp} = 6.84$ and 7.75 ks, respectively, corresponding to the $0.4\text{MJ}/\text{m}^2$ data point in Figure 8, near the optimum $1\text{MJ}/\text{m}^2$ fluence value. Pulse duration was 4.5ns.

the same fluence for maximum ablation efficiency as was observed in the Au data [$1\text{MJ}/\text{m}^2$].

Al data [Figure 9] was not as complete as the Au data because the $1\text{-}2\mu\text{m}$ thickness of the Al coatings did not permit reaching the higher intensities before coating burnthrough occurred.

We irradiated one track on the gold target disk for 40 minutes to see whether the bottom of the feature created would be too rough to maintain focus. Microscopic examination showed that the irradiated surface was smoother than the original surface. The rms roughness could not be directly determined, but was better than $\pm 1\mu\text{m}$.

SUMMARY AND CONCLUSIONS

We measured, for the first time, the thrust developed when ns-duration, repetitive laser pulses are directed at a metal target material in vacuum in a completely self-contained thruster device. To do the measurements with our laboratory lasers, it was necessary to measure (for the first time) thrusts as small as 100nN with 25% accuracy using a new type of thrust stand that we invented for the measurements.

We showed that a ns-pulse laser-driven microthruster can reach I_{sp} values in excess of 3ks on a sustained basis, and that I_{sp} can be adjusted over a decade by varying laser intensity.

We measured ablation efficiencies up to 100% with passive (nonexothermic) metallic targets. These were gold and aluminum coatings applied to a 2.5-inch IBM hard drive disk. Electroplated Au coatings were thicker than the Al coating that could be applied by ion sputtering, with the result that burnthrough prevented taking Al data at the highest intensities employed.

We measured ion velocities using specialized TOF detectors. The simple shape of the detected signals (no multiple peaks) at moderate laser fluence indicated that the TOF signal is produced by a single ion type and a single ion charge state. At higher fluences, we see double-humped TOF signals, which may be due to two different charge states, or due to the plasma clamping phenomenon [9].

The excellent agreement we observed between I_{sp} deduced from the $C_m Q^*$ product and from ion velocity v_i near the optimum fluence of $1\text{MJ}/\text{m}^2$ tells us that most of the thrust at that fluence is generated by ions, rather than neutrals. The divergence between these two I_{sp} parameters at higher intensity with Au, and at all intensities for

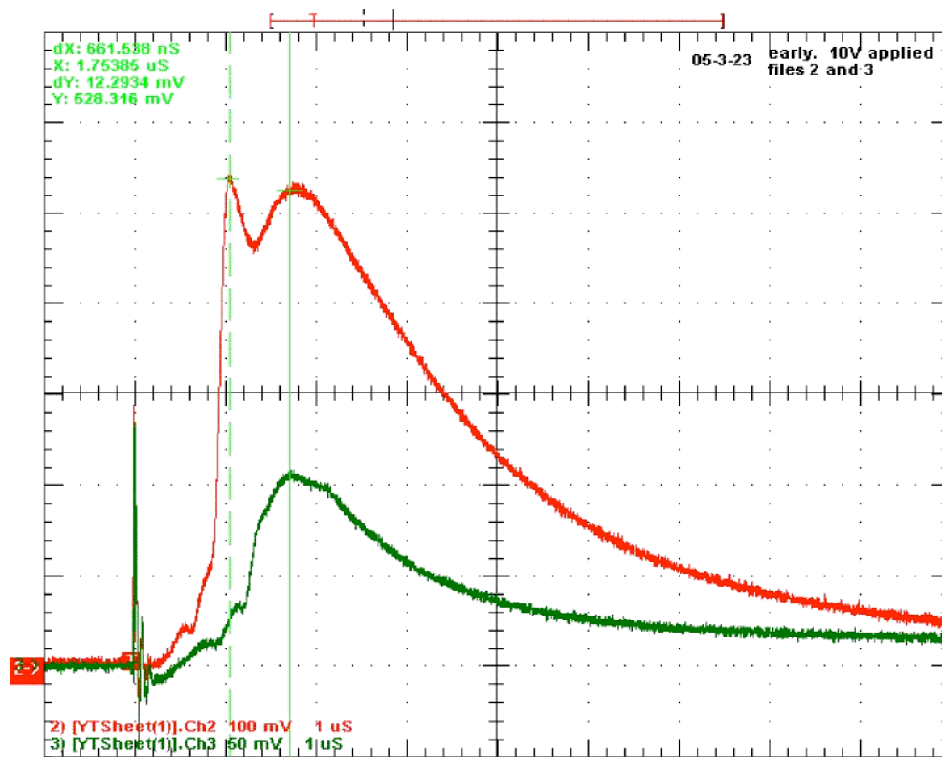


Figure 7. High fluence TOF Detector Trace (-10V bias, Au Target) shows ion speed $79\text{km}/\text{s}$ at the half-height of the rise in the main feature. This corresponds to ion $I_{sp} = 8.07\text{ks}$. Unlike the moderate-fluence picture in Figure 8, the TOF distribution has a definite second feature. For this shot, laser fluence on target was $21\text{MJ}/\text{m}^2$ [above the optimum $1\text{MJ}/\text{cm}^2$ fluence value], and pulse duration was 4.5ns .

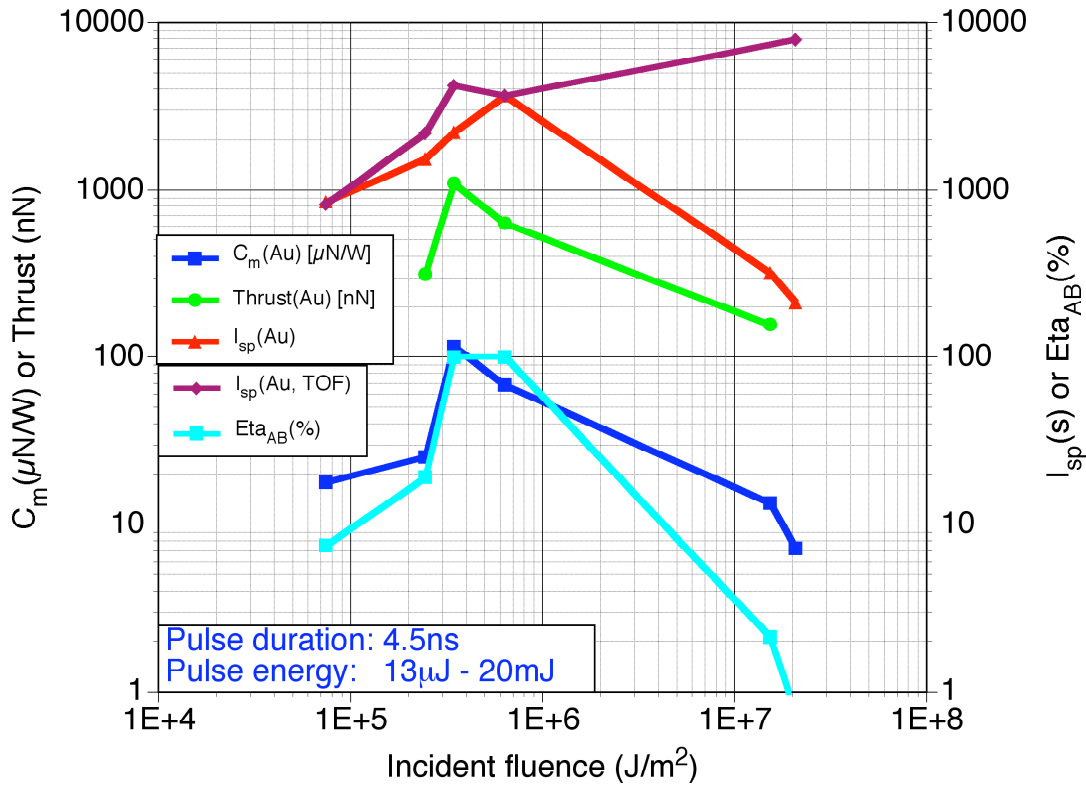


Figure 8. Experimental data for Au target vs. incident fluence. Ablation efficiency approaches 100% near 1MJ/m². Thrust as small as 150nN was measured reliably. C_m ranged between 10 and 100 μN/W. Specific impulse based on measured mass loss was as large as 3,700 seconds, and could be varied between 0.2 and 3.7 ks by varying incident intensity. I_{sp} based on ion TOF measurements agrees roughly with I_{sp} from mass loss up to 0.8MJ/m², but the two trends diverge at higher intensity, as ablation efficiency drops to the 1% level.

our Al measurements, suggests plasma clamping, a phenomenon in which, above a certain threshold, laser-produced plasma self-regulates its optical transmission in such a way that the fluence transmitted to the surface is constant, independent of incident fluence. This phenomenon will give an initial burst of high-energy ions, but a much lower energy exhaust during the rest of the laser pulse, and could explain the double-humped feature in Figure 7.

There are two other possible reasons for double-humped TOF distributions: a) exciting metal ions to more than one charge state, and b) Surface cleaning of water vapor in the early part of a data run. We have occasionally seen this effect. Possibility a) could not be tested because we did not have charge state diagnostics.

These two I_{sp} features, which we might call realistic vs. theoretical I_{sp}, remind us that many reports in the literature of very high I_{sp} values based on ion velocities alone must be taken with a grain of salt. Ours are the first results reported in the literature in which I_{sp} was actually measured from mass loss, and the C_mQ* product compared with

measured ion velocities under the same conditions in the same experiment at appropriate background pressure for measuring ion velocities via TOF. It is also the first in which an optimum fluence for high I_{sp} was shown.

The fluence for which these two types of I_{sp} were found to agree, 1MJ/m^2 , was predicted by simulations reported in reference 10. This fluence corresponds to 1mJ incident on a $35\text{-}\mu\text{m}$ spot diameter. This establishes the operating parameters for the fiber laser we would use for a space-qualified microthruster. A pulse energy of 1mJ at 16kHz , producing 8W average power and $80\mu\text{N}$ thrust, is now very achievable in fiber laser technology, and such a spot size would be easy to achieve with a relatively long focal length lens.

We operated the microthruster for 7 hours on our gold disk target, using about 20% of the target surface, but only about 2% of the target material, which was originally deposited on the disk in a $20\text{-}\mu\text{m}$ -thick coating. The disk drive operated at

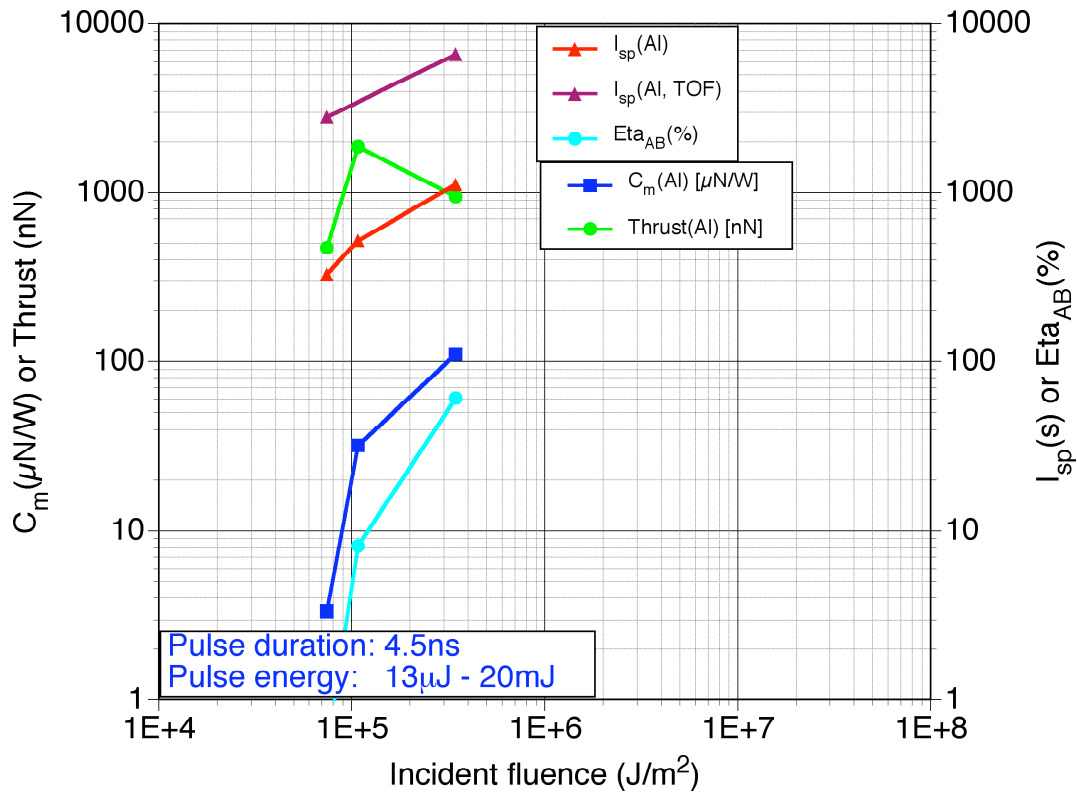


Figure 9. Experimental data for Al target vs. incident fluence. Ablation efficiency approaches 100% near 0.5MJ/m^2 . C_m ranged between 5 and $100\mu\text{N/W}$. Specific impulse based on measured mass loss was as large as 1,100 seconds. I_{sp} based on ion TOF measurements did not agree with I_{sp} from mass loss up to 0.5MJ/m^2 , being much larger for the entire range studied. Higher fluences could not be studied because of Al coating burnthrough.

4200 rpm for 10.4 hours in vacuum without special preparation, and without any degradation in performance. However, this is not the target delivery mechanism we would propose for a space-qualified ns-pulse microthruster.

Taken together, these results demonstrate the feasibility of a ns-pulse laser-driven microthruster, and provide the first data on performance of such a device.

REFERENCES

1. Phipps, C. R. and Luke, J. R., "Diode Laser-driven Microthrusters: A new departure for micropropulsion," *AIAA Journal* **40** no. 2 2002, pp. 310-318
2. Phipps, C. , Luke, J., Lippert, T., Hauer, M. and Wokaun, A., "Micropropulsion using a Laser Ablation Jet," *J. Propulsion and Power*, **20** no. 6, 2004, pp. 1000-1011
3. F. di Teodoro, J. P. Koplow and S. W. Moore, "Diffraction-limited, 300-kW peak-power pulses from a coiled multimode optical fiber," *Opt. Lett.* **27**, pp. 518-520 (2002) plus private communications.
4. D. A. Gonzales and R. P. Baker, "Microchip Laser Propulsion for Small Satellites," paper AIAA 2001-3789, 37th AIAA/ASME/SAE/ASEE Joint Propulsion Conference, Salt Lake City (2001)
5. C. R. Phipps, "Advantages of using ps-pulses in the ORION Space Debris Clearing System", *Proc. International Conference on Lasers 97*, STS Press, McLean, VA (1998) pp. 935-941
6. D. A. Gonzales and R. P. Baker, "Micropropulsion using a Nd:YAG microchip laser," *Proc. SPIE Conference on High Power Laser Ablation IV*, **SPIE 4760**, pp. 752-765 (2002)
7. C. R. Phipps and M. M. Michaelis, "Laser Impulse Space Propulsion," *Laser and Particle Beams*, **12** (1), 23-54 (1994)
8. D. W. Gregg and S. J. Thomas, "Kinetic Energies of Ions Produced by Laser Giant Pulses", *J. Appl. Phys.* **37**, 4313-16 (1966)
9. J. F. Figueira, S. J. Czuchlewski, C. R. Phipps, Jr., and S. J. Thomas, "Plasma-Breakdown Retropulse Isolators for the Infrared," *Appl. Opt.* **20**, 838 (1980).